Evidence for an autonomous 5′ target recognition domain in an Hfq-associated small RNA

Kai Papenfort[a,b,1], Marie Bouvier[b,1], Franziska Mika[b,1], Cynthia M. Sharma[a,b], and Jörg Vogel[a,b,2]

[a]Institute for Molecular Infection Biology, University of Würzburg, D-97080 Würzburg, Germany; and [b]RNA Biology Group, Max Planck Institute for Infection Biology, D-10117 Berlin, Germany

Edited* by Carol A. Gross, University of California, San Francisco, CA, and approved October 18, 2010 (received for review July 6, 2010)

The abundant class of bacterial Hfq-associated small regulatory RNAs (sRNAs) parallels animal microRNAs in their ability to control multiple genes at the posttranscriptional level by short and imperfect base pairing. In contrast to the universal length and seed pairing mechanism of microRNAs, the sRNAs are heterogeneous in size and structure, and how they regulate multiple targets is not well understood. This paper provides evidence that a 5′ located sRNA domain is a critical element for the control of a large posttranscriptional regulon. We show that the conserved 5′ end of RybB sRNA recognizes multiple mRNAs of *Salmonella* outer membrane proteins by ≥7-bp Watson–Crick pairing. When fused to an unrelated sRNA, the 5′ domain is sufficient to guide target mRNA degradation and maintain σ^E-dependent envelope homeostasis. RybB sites in mRNAs are often conserved and flanked by 3′ adenosine. They are found in a wide sequence window ranging from the upstream untranslated region to the deep coding sequence, indicating that some targets might be repressed at the level of translation, whereas others are repressed primarily by mRNA destabilization. Autonomous 5′ domains seem more common in sRNAs than appreciated and might improve the design of synthetic RNA regulators.

envelope stress | multiple targeting | noncoding RNA | porin

Small RNAs that act on *trans*-encoded target mRNAs by short base pairing are important posttranscriptional regulators in many organisms. The two most abundant classes to date are the microRNAs of eukaryotes and the Hfq-associated small regulatory RNAs (sRNAs) of gram-negative bacteria such as *Escherichia coli* and *Salmonella* (1). The ∼22-nt microRNAs use well-established mechanisms and machinery to repress mRNAs by short seed pairing within the 3′ UTR, and a single microRNA might regulate hundreds of genes in parallel (2).

The bacterial sRNAs are also increasingly found to control multiple targets, although by binding the 5′ region of bacterial mRNAs (3). In fact, some sRNAs have an impact on dozens of genes under stress or altered growth conditions (4–7), with target sites being known for a subset of the regulated mRNAs. The Sm-like protein, Hfq, is required for intracellular stability and target annealing of the sRNAs (1, 8). Global analyses of Hfq-bound transcripts suggest an excess of potential targets over regulators (9, 10), further arguing that multiple targeting might be the general mode of sRNA action.

Unlike the universal length and seed pairing of microRNAs, there are few common denominators for Hfq-dependent regulators. The sRNAs dramatically vary in size (50–250 nt) and secondary structure (11), and sRNA-mRNA interactions range from >30-bp duplexes in MicF-*ompF* or Spot42-*galK* (12, 13) to only 6 bps that are critical in SgrS-*ptsG* (14). Most of the sRNAs analyzed to date inhibit translational initiation of targets by sequestering the Shine–Dalgarno (SD) or start codon (AUG) sequences of the ribosome binding site (RBS); how the recognition of these conserved RBS elements would ensure highly specific target selection is little understood (15). Interestingly, there are a few recent examples of sRNA binding upstream or downstream of SD/AUG sequences (16–21), suggesting that the mRNA window for target repression could be broader than the RBS. Emerging evidence suggests that those sRNA nucleotides interacting with multiple targets might be maintained by selection (18) and often cluster in the 5′ sRNA region (6, 16, 20, 22–24).

The ∼80-nt RybB sRNA was recently shown to accelerate mRNA decay of many major and minor outer membrane proteins (OMPs) in *Salmonella* and *E. coli* (25, 26). RybB is activated by the alternative σ^E factor when excessive OMP synthesis or envelope damage causes periplasmic folding stress (25–28). As such, RybB is a major facilitator of σ^E-directed global OMP repression (25, 29) and is required for envelope homeostasis and feedback regulation of σ^E (25, 27).

Pulse expression of *Salmonella* RybB reduces the half-lives of stable *omp* mRNAs from of ≥10 min to ∼1 min (25), and both RybB and its putative targets interact with Hfq (10), all of which predicts direct regulation by RNA interactions. Biocomputational algorithms failed to predict statistically significant RybB pairing with the RBS of targets (25), however, and the only known RybB site thus far was discovered in the coding sequence of *Salmonella ompN* mRNA (17).

Here, we report genetic evidence that the conserved 5′ end of RybB constitutes an autonomous multiple-target binding domain used to select many *omp* mRNAs by short (≥7 bp) Watson–Crick pairing. This domain is essential and sufficient for target repression and adjusting σ^E activity. RybB sites in *omp* mRNAs are associated with a unique 3′ adenosine signal and are located in a broad window ranging from 5′ located stability elements into the deep coding sequence, suggesting varying contributions of translational inhibition and mRNA decay to target repression. An autonomous 5′ domain might be more common in sRNAs than appreciated and also governs the prototypical MicF-*ompF* regulation.

Results

OMP Depletion by Constitutive RybB Expression. RybB effects have been studied at the *omp* mRNA level following short expression of the sRNA (25, 26). To assay regulation at the protein level, we used the constitutive expression plasmid pP_L-RybB (17), which confers equivalent RybB levels throughout growth (Fig. 1) and approximately fivefold more than the chromosomal *rybB* gene after σ^E induction (*SI Appendix*, Fig. S1). We observed full depletion of three 30- to 35-kDa proteins—OmpA, OmpC, and OmpD—known as the most abundant *Salmonella* porins during regular growth (Fig. 1). Depletion of the fourth major porin, OmpF, was confirmed using strains with individual *omp* gene disruptions (*SI Appendix*, Fig. S2). In contrast, there was no effect on the OmpX porin (Fig. 1) whose mRNA is refractory to RybB in *Salmonella* (25), suggesting that repression was specific and not caused by a general block of OMP biogenesis. Because constitu-

Author contributions: K.P., M.B., F.M., C.M.S., and J.V. designed research; K.P., M.B., F.M., and C.M.S. performed research; K.P., M.B., F.M., C.M.S., and J.V. analyzed data; and K.P. and J.V. wrote the paper.

The authors declare no conflict of interest.

*This Direct Submission article had a prearranged editor.

Freely available online through the PNAS open access option.

[1]K.P., M.B., and F.M. contributed equally to this work.

[2]To whom correspondence should be addressed. E-mail: joerg.vogel@uni-wuerzburg.de.

This article contains supporting information online at www.pnas.org/lookup/suppl/doi:10.1073/pnas.1009784107/-/DCSupplemental.

GENETICS

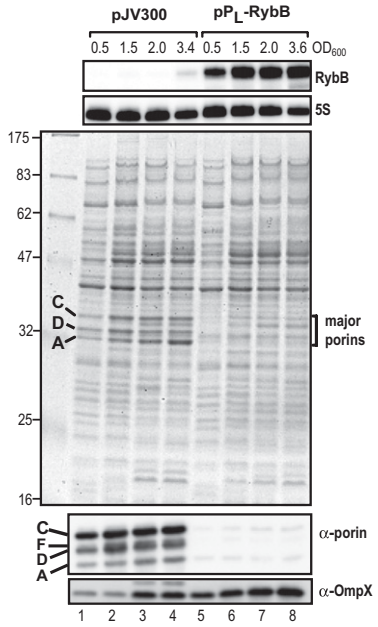

Fig. 1. Constitutive RybB expression causes porin depletion in *Salmonella*. RNA and protein samples were prepared from WT *Salmonella* carrying plasmids pJV300 (empty vector; lanes 1–4) or pP_L-RybB (lanes 5–8) after growth to exponential phase (OD_{600} of 0.5) or stationary phase (OD_{600} of 1.5, 2, or 3.4). (*Top*) Autoradiograms of a Northern blot probed for RybB or 5S rRNA (loading control). (*Middle*) Coomassie-stained SDS gel of corresponding total protein. The major OmpA/C/D porin bands are labeled. (*Left*) Comigrating marker proteins; sizes are expressed in kilodaltons. (*Bottom*) Western blot using antisera against major porins or OmpX (control) as indicated.

tive RybB expression did not affect bacterial growth rate or viability, it lent itself to genetic dissection of RybB target pairing.

5′ Domain of RybB Regulates Multiple *omp* mRNAs. Alignment of RybB homologs of diverse γ-proteobacterial species revealed that this sRNA possesses an exceptionally well-conserved 5′ end (17). Moreover, we previously obtained evidence that RybB nucleotides 1–16, dubbed R16 (Fig. 2*A* and *SI Appendix*, Fig. S3), are sufficient for base pairing and repression of *ompN* mRNA (17). To this end, we grafted R16 onto either of two control sRNAs, TMA or TOM; the resulting chimeric sRNAs, R16TMA or R16TOM (Fig. 2*B*), repressed *ompN* invariably from wild-type (WT) RybB (17).

To determine whether R16 also regulated other targets, we assayed effects of R16TMA or R16TOM and of a previously undescribed 5′ deleted variant of RybB (Δ1–9; Fig. 2*B*) on the accumulation of abundant OMPs (Fig. 2*C*, *Top*). Both R16TMA and R16TOM down-regulated the major OMPs (lanes 4–5), whereas their parental TMA and TOM RNAs did not (lanes 6–7), suggesting a broader role of R16 in OMP repression. The Δ1–9 truncation rendered RybB unable to deplete major OMPs (lane 3), corroborating that an intact 5′ end is pivotal to regulation. Importantly, all tested sRNAs were transcribed from the same constitutive promoter as in pP_L-RybB and accumulated to comparable levels in vivo (*SI Appendix*, Fig. S4). Thus, RybB-mediated OMP repression is stringently correlated with the presence of the R16 sequence.

Bacterial sRNAs typically target the SD or AUG sequence, which can be assayed in vivo using a well-established translational *gfp* reporter system (30). We constructed reporter plasmids for eight RybB targets (Fig. 2*C* and *SI Appendix*, Fig. S5), fusing the 5′ UTR and up to 21 codons to the NH_2 terminus of GFP. All fusions are constitutively transcribed to score specifically for posttranscriptional regulation. Reporters were individually combined in *Salmonella* with the above WT or mutant RybB plasmids, and regulation of the fusion proteins was determined by Western blot analysis (Fig. 2*C*, *Bottom*).

Wild-type RybB repressed all target fusions (Fig. 2*C*, lane 2), predicting that the cloned mRNA regions contained a RybB target site; these repressions were specific because RybB did not regulate *gfp* alone or an *ompX::gfp* control fusion. As with the major OMPs, the RybBΔ1–9 variant did not regulate any of the fusions (Fig. 2*C*, lane 3). In contrast, R16TMA and R16TOM down-regulated all fusions (Fig. 2*C*, lanes 4 and 5) to the same degree as WT RybB; we attributed these regulations to R16 because the parental control RNAs (TMA and TOM) alone had no impact on reporter activity (Fig. 2*C*, lanes 6 and 7). Together, these results narrowed down the sequence space for the prediction of RybB binding.

RybB Target Sites in *omp* mRNAs. We used the *RNAhybrid* algorithm (31) to predict RNA duplexes of R16 with the above cloned 5′ target mRNA fragments. Fig. 3*A* shows the highest scoring interaction for each target, all of which have a change in free energy ($\Delta G°$) in a −24.2 to −18.8 kcal/mol^{-1} range, similar to the known RybB-*ompN* pairing (included for comparison) yet far more favorable than the −13 to −8 kcal/mol^{-1} range expected for random RNA pairing (15). Intriguingly, each interaction involves 5′ terminal pairing of RybB, commonly of seven or more consecutive Watson–Crick pairs.

The RybB target sites are strikingly diverse in relative mRNA position (Fig. 3*A*). Canonical binding sites overlapping SD/AUG must fall within a −16 to +3 window on mRNA (+1 is A of the start codon AUG); only *tsx* would be targeted so. Unexpectedly, RybB would recognize the majority of targets in the coding sequence (*fadL*, *ompA*, *ompD*, *ompN*, *ompS*, and *ompW*) or far upstream of the RBS (*ompC* and *ompF*). We used a previously published RybB-M2 mutant (17) carrying a $C_2 \rightarrow G$ change to validate the six most representative interactions (Fig. 3*B*). Quantitative single-cell measurements of *gfp* reporter activity using FACS showed that, as expected, the M2 point mutation disrupting the 5′ helix of RybB-target duplexes (Fig. 3*A*) consistently abrogated target regulation (Fig. 3*B*, *Left*). Reciprocally, we constructed compensatory M2' alleles of all six target fusions, seeking restoration of base pairing (Fig. 3*A*; G→C change at positions −42, −39, −8, +19, +31, and +49 in *ompC*, *ompF*, *tsx*, *ompW*, *ompA*, and *fadL*, respectively). In line with our predictions, the M2' reporters were insensitive to WT RybB but regulated by RybB-M2 sRNA (Fig. 3*B*, *Right*). Including *ompN* pairing (17), seven RybB-*omp* interactions are now firmly validated in vivo.

5′ End of RybB Is an Autonomous Regulatory Domain. Next, we asked whether the short R16-target duplexes were sufficient to repress native *omp* mRNAs in the σ^E response. To this end, we replaced the chromosomal RybB sequence with the R16TMA chimera while keeping the σ^E-dependent promoter of the *rybB* locus. Northern blots showed that following σ^E induction, WT RybB and R16TMA accumulated to comparable levels. Importantly, the chromosomally encoded R16TMA RNA down-regulated the native *ompC/D/F/N/S* target mRNAs with almost identical kinetics as did WT RybB, demonstrating that R16-mediated pairing is sufficient for target repression under physiological conditions (Fig. 4*A*).

We and others have reported that Δ*rybB* strains suffer chronic envelope stress as judged by elevated σ^E activity even under standard growth conditions, likely attributable to excessive OMP synthesis in the absence of RybB (25–27). To test whether R16 could counteract envelope stress on its own, we compared the levels of *rpoE* and *degP* mRNA, two sensitive markers of σ^E induction (29), among *Salmonella* WT, Δ*rybB*, and R16TMA strains at stationary phase. Fig. 4*B* shows that R16TMA fully reversed the twofold (*degP*) or 7.5-fold (*rpoE*) increase of these σ^E-dependent transcripts to WT levels. Next, we used a *gfp* reporter fusion to the highly σ^E-dependent *rybB* promoter (25) to assay envelope stress over growth (Fig. 4*C*). Samples taken at five points from late exponential through stationary phase consistently showed several-fold increased *rybB-gfp* reporter activity, hence chronic σ^E induc-

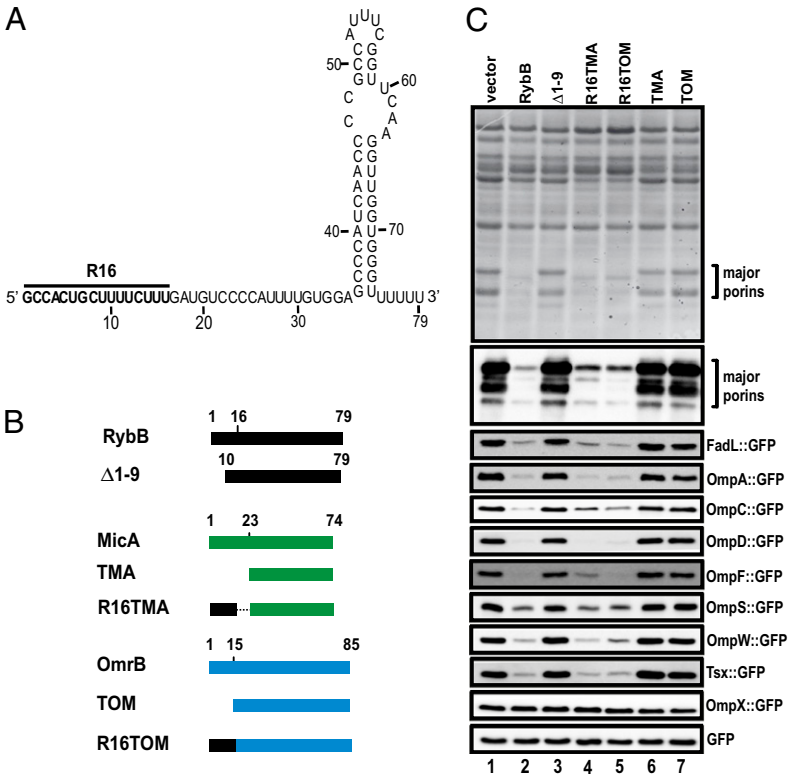

Fig. 2. First 16 nucleotides of RybB are sufficient for porin repression. (*A*) Structure of *Salmonella* RybB RNA based on alignment in *SI Appendix*, Fig. S3 and probing (17). A horizontal bar denotes the R16 sequence. (*B*) Schematic drawing and color code explaining the origin of chimera RNAs (R16TMA and R16TOM) and control RNAs (TMA and TOM) from *Salmonella* RybB, MicA, and OmrB. (*C*) Comparison of target regulation in a *Salmonella* Δ*rybB* strain transformed with pJV300 (lane 1) or pP_L-RybB (lane 2) or in plasmids expressing the following RybB mutants from a P_L promoter: Δ1–9 (lane 3); R16TMA or R16TOM, which carry the R16 sequence (lane 4 or 5); and their parental control RNAs, TMA (5′ truncated MicA; lane 6) or TOM (5′ truncated OmrB; lane 7). (*Upper*) Bacteria were cultured to an OD_{600} of 2.0, and major porin regulation was determined on a stained SDS gel (first panel) or by Western blot analysis (second panel). (*Lower*) Western blot analysis of regulation of translational *gfp* fusions to the 5′ regions of RybB target mRNAs (*fadL*: −100/+63 relative to AUG, *ompA*: −133/+45, *ompC*: −79/+36, *ompD*: −66/+36, *ompF*: −112/+36, *ompS*: −66/+36, *ompW*: −29/+36, *tsx*: −76/+36) or to *ompX::gfp* or *gfp* control vectors (*SI Appendix*, Fig. S5). (*Right*) Abundance of GFP fusion proteins was assayed after overnight growth for 12 h. The *ompA::gfp* fusion was analyzed in an *E. coli* Δ*rybB* strain.

tion, in Δ*rybB* vs. WT *Salmonella*. In contrast, the σ^E activity in the R16TMA strain was indistinguishable from WT, suggesting full complementation. These results establish that the conserved R16 sequence is sufficient to control a global regulatory circuit under the conditions tested.

Discussion

Bacterial antisense regulation was traditionally associated with the extended base-pairing potential of *cis*-antisense RNAs transcribed opposite to a single target gene in plasmids and mobile genetic elements (32). Although structural analyses have revised the concept of long RNA duplexes (33, 34), few *cis*-antisense RNAs are found in sufficiently diverse bacteria to predict important RNA nucleotides by hint of sequence conservation. In contrast, Hfq-dependent sRNAs often act on multiple targets and carry short stretches of sequence conserved in a wider range of species. These characteristics have allowed us to identify R16 as a 5′ located functional domain that comprises ∼20% of RybB (Fig. 2*A*) and can act autonomously to control a functionally related yet structurally diverse family of mRNAs as well as the overall state of the cell (Fig. 4).

A survey of conservation patterns and target pairing of 18 well-characterized *E. coli*/*Salmonella* sRNAs shows that more than a third of them possess a conserved 5′ end and act by 5′ terminal pairing (*SI Appendix*, Figs. S6 and S7 and Table S1). Intriguingly, enrichment of conserved nucleotides toward the 5′ end was most prominent in MicF, the founding member of the class of *trans*-acting antisense RNAs (35). Similar to RybB, the conserved 5′ end of MicF is sufficient for target repression when fused to TMA RNA, suggesting that MicF also carries an autonomous 5′ target-binding domain (*SI Appendix*, Fig. S6). The principles of target recognition by 5′ terminal pairing sRNAs such as RybB and of the modular structure of sRNAs in general could facilitate the design of artificial regulators for the control of synthetic regulatory circuits.

Structure of RybB Target Sites. Recent work has implicated conserved 5′ nucleotides in target pairing of several Hfq-dependent sRNAs (6, 16, 20, 22–24). For example, mutation in the 5′ region of the highly similar OmrA/B sRNAs impaired repression of several *E. coli* mRNAs under conditions of sRNA overexpression, prompting complementarity searches with this region to predict an additional OmrA/B target (22). However, whether the involved 5′ nucleotides sufficed for regulation under physiological conditions or needed to partner with other sRNA regions for productive target recognition remained unknown.

Our data suggests that target selection by RybB is fully determined by short 5′ terminal Watson–Crick pairing (Fig. 3*A*). First, sRNA chimeras carrying the R16 sequence (R16TMA and R16TOM) regulate targets almost indistinguishably from WT RybB. Second, σ^E-induced chromosomal RybB and R16TMA RNAs promote the same *omp* mRNA decay (Fig. 4); thus, R16 suffices for target recognition under native expression conditions. Third, the M2 point mutation at the second RybB position abrogates repression (Fig. 3) even if the typically short 5′ helix is followed by strong downstream pairing as in RybB-*ompN* (17) (Fig. 3*A*).

Conservation patterns in mRNAs further argue that target recognition is restricted to short 5′ terminal pairing of RybB. For example, alignment of enterobacterial *ompC* sequences reveals conservation of 5′ UTR nucleotides −50 to −41 complementary to RybB nucleotides 1–9 (Fig. 5*A*). Although the adjacent *ompC* nucleotides are conserved as well, they do not extend the RybB-*ompC* helix (Figs. 3*A* and 5*A*), suggesting counterselection of long pairing. Similar patterns mark RybB sites in other *Salmonella* *omp* mRNAs (*SI Appendix*, Fig. S8).

The target sites in mRNAs share little sequence except for the four nucleotides recognized by the extreme 5′ end of RybB. However, almost all RybB sites are followed by an unpaired adenosine (Fig. 5*C*), and this 3′ adenosine signal is also observed with other 5′ terminal pairing sRNAs (Fig. 5*D*). Thus, despite radical differences in underlying machinery and mechanisms of target regulation, some features of bacterial 5′ pairing sRNAs are reminiscent of animal microRNAs, which select multiple targets by short Watson–Crick pairing of a 5′ located conserved "seed" (microRNA nucleotides 2–7), flanked by 3′ adenosine in the target (2, 36). Because these features are instrumental in the discovery of microRNA target sites, extra scores for conserved

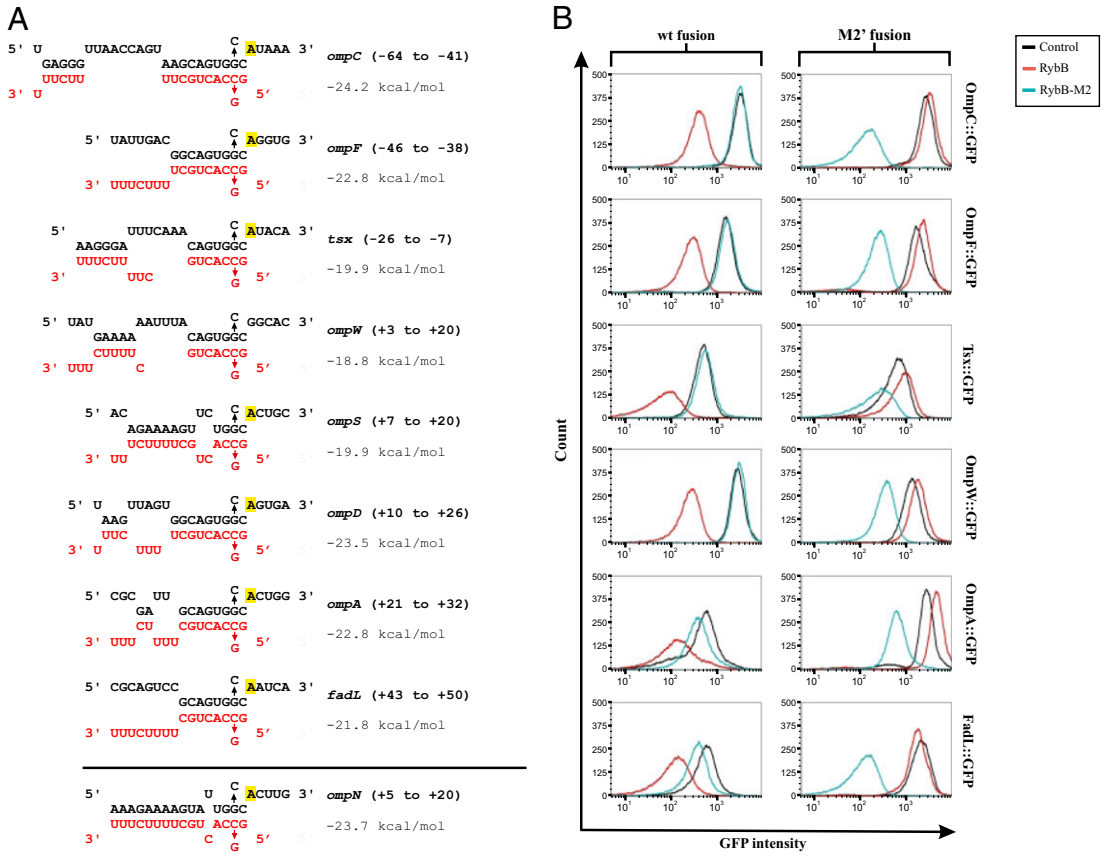

Fig. 3. RybB target sites on *omp* mRNAs. (*A*) Antisense complementarity of R16 (red) with the above tested *omp* mRNA fragments (black) predicted by *RNAhybrid,* sorted by relative position to the AUG start codon. The RybB-*ompN* pairing (17) is shown for comparison. Numbers in parentheses denote mRNA nucleotides relative to AUG (A is +1); the predicted change in free energy of an interaction is given below. Vertical arrows denote the $C_2 \rightarrow G$ mutation in RybB-M2 RNA and the compensatory G→C change in M2′ mRNA alleles. The 3′ adenosine flanking most RybB sites is marked in yellow. (*B*) Validation of selected interactions. Stationary phase *Salmonella* Δ*rybB* cells carrying *gfp*-target fusions in combination with RybB expression or control plasmids were analyzed by FACS. Results are plotted in fluorescence histograms derived from 30,000 events per sample. Cellular fluorescence is given in arbitrary units (GFP intensity). Histograms on the same line represent the WT or M2′ mutant fusions of the same target. Each fluorescence histogram represents triplicate results from pPL-RybB (red), pPL-RybB-M2 (blue), or pJV300 (black) samples.

sRNA domains and a 3′ adenosine might help to improve target predictions in bacteria.

Mechanisms of mRNA Regulation by RybB. Translational interference on the basis of sRNA complementarity to SD or AUG was proposed to serve as the primary mechanism of target repression (37), irrespective of concomitant mRNA degradation by recruitment of RNase E (38), which should relax the RBS dependence. A stringent requirement to target the conserved RBS elements is difficult to reconcile with sRNAs having to discrim-

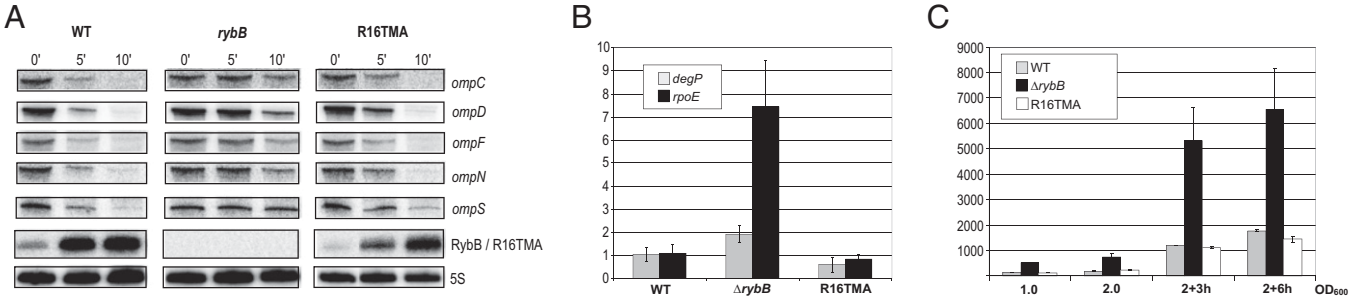

Fig. 4. Chromosomal R16 is sufficient to repress *omp* mRNAs in the σ^E response. The transcribed region of *Salmonella rybB* was chromosomally replaced with the R16TMA sequence. (*A*) WT, Δ*rybB*, and R16TMA strains were transformed with a pBAD-RpoE plasmid. Levels of *omp* mRNAs before or following arabinose induction of σ^E at exponential phase for 5 and 10 min were analyzed on Northern blots. RybB/R16TMA expression was detected with an LNA probe for the R16 sequence. (*B*) WT, Δ*rybB*, and R16TMA strains were grown to late stationary phase (OD_{600} of 3), and the relative expression of two σ^E-responsive genes (*rpoE* and *degP*) was determined by quantitative RT-PCR. RNA levels in WT are set to 1. (*C*) Reporter activity (arbitrary fluorescence values) of the above strains but carrying a *gfp* fusion to the σ^E-dependent *rybB* promoter was determined at indicated stages of growth.

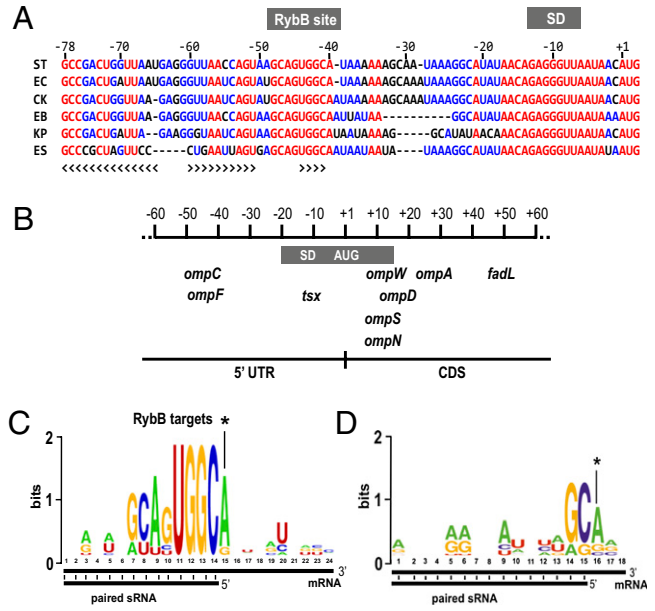

Fig. 5. Conservation and distribution of RybB target sites. (*A*) Alignment of *ompC* 5′ UTRs of various enterobacteria (abbreviations given in *SI Appendix*, Fig. S3). Gray boxes indicate the conserved SD sequence and RybB target site. Inverted arrows indicate the 5′ hairpin. Red, blue, or black coloring indicates strong, medium, or weak conservation, respectively. (*B*) Approximate positions of RybB sites in *omp* target mRNAs. Most RybB targets are recognized in the coding sequence, and core binding generally occurs outside the canonical SD/AUG region. Local alignment of RybB target mRNAs (*C*) or targets regulated by other 5′ end-pairing sRNAs (*D*) (*SI Appendix*, Fig. S8). Graphs were generated using Weblogo (http://weblogo.berkeley.edu/logo.cgi).

inate genuine targets from thousands of cellular messengers (39). Intriguingly, the RybB sites determined here reveal almost no tight contacts with SD or AUG (Figs. 3*A* and 5*B*). Instead, RybB operates within a >100-nt window around AUG, which is much larger than the −20/+15 window for general antisense inhibition of initiating 30S ribosomes previously suggested by structural and in vitro interference data (17, 40–42). Thus, during its evolution toward a global regulator, RybB might have selected the most suitable pairing region in the diverse *omp* targets, likely at the expense of stringent translational control. In other words, current models predict efficient competition of RybB with ribosomes for the *tsx* (SD sequestration) and *ompD*/*N*/*S*/*W* targets ["five-codon window" in the 5′ proximal coding sequence (17)].

In contrast, four RybB sites lie well outside the 30S contacts, either in the 5′ UTR (*ompC* and *ompF*) or in the coding sequence downstream of the fifth codon (*ompA* and *fadL*). Pairing in the deep coding sequence is unlikely to abrogate translation because elongating 70S ribosomes unwind RNA duplexes much stronger than RybB-*fadL* or RybB-*ompA* (43). Of note, MicC sRNA was recently shown to repress *Salmonella ompD* mRNA at codons 23–26 without 30S or 70S inhibition but induced RNase E-dependent decay (16). Similarly, we find that RybB requires RNase E for repression in the deep coding sequence (*SI Appendix*, Fig. S9), suggesting that RybB acts on *fadL* and *ompA* by alternative gene silencing downstream of translational initiation similar to MicC-*ompD* (16).

RybB pairing upstream of the *ompC* and *ompF* RBS could involve translational repression, induced mRNA decay, or both. 30S inhibition at such distal sites was recently reported for Hfq-dependent regulators: GcvB targets a translational enhancer element of *gltI* mRNA (18), RyhB targets a leader peptide of *fur* (19), and OmrAB targets a conserved RNA structure element of *csgD* (20). None of these models readily applies here, and possible translational control of *ompC* and *ompF* is currently being investigated. However, we note that RybB binds within a conserved 5′ hairpin of *ompC* mRNA (Fig. 5*A*). Such hairpins commonly stabilize bacterial messengers by impeding 5′ pyrophosphorylation and RNase E-mediated degradation (44, 45). Thus, RybB pairing to the 3′ flank of the *ompC* hairpin (−64 to −41) might impair full formation of this stability element to promote the accelerated *ompC* mRNA decay that follows σ^E induction (25, 26, 29). Altogether, the non-RBS sites support the emerging importance of induced mRNA decay in Hfq-dependent regulations (38, 46). Moreover, recent work on Hfq-dependent regulations involving RNase E showed that diverse sRNAs undergo coupled degradation with their targets (47, 48). In the case of RybB, such concomitant consumption of the sRNA with *omp* mRNAs would permit fast recovery of OMP synthesis once the σ^E-inducing envelope stress is alleviated.

Modular sRNA Structure and Implications for Synthetic Design. Our key finding is that the 5′ end of RybB constitutes an autonomous target recognition domain that, on transfer to another sRNA, suffices to both control many OMPs and suppress activation of the σ^E response over growth (Fig. 4). The σ^E regulon is complex, comprising ~100 genes (28, 29), and R16 can be predicted biocomputationally (31) to target additional mRNAs with σ^E-related functions. Interestingly, the other σ^E –dependent sRNA, MicA, also uses conserved 5′ proximal nucleotides to select multiple mRNAs (26, 49–52).

Despite its small size and simple structure, RybB now appears to carry three distinct modules: (*i*) a specificity domain (R16) determining the target range, and thus physiological activity; (*ii*) an A/U-rich Hfq site (53) in the 30-nt region for general target annealing; and (*iii*) a ρ-independent terminator required for the biogenesis and stability of this global regulator. We believe that knowledge of modular sRNA structure will permit better design of synthetic antisense regulators, a task pioneered for single genes more than 3 decades ago (54). Indeed, substitution of R16 with a complementary sequence of a generic mRNA successfully generated a unique regulator (17). The very short 5′ terminal pairing and relaxed position dependence of target sites revealed in this study might now be exploited for reprogramming of regulatory circuits or metabolism through multiple targeting with a synthetic 5′ end of RybB.

Experimental Procedures

Oligonucleotides, Plasmids, Bacterial Strains, and Growth. Bacterial strains and their construction details are listed in *SI Appendix*, Table S2. Strains were grown at 37 °C in LB or on LB plates. Ampicillin (100 μg/mL), kanamycin (50 μg/mL), chloramphenicol (20 μg/mL), and L-arabinose (0.2%) were added where appropriate. *Salmonella* WT (SL1344) or mutant strains were transformed with plasmids by electroporation as described (55). DNA, LNA (locked nucleic acid), and RNA oligonucleotides as well as plasmids are listed in *SI Appendix*, Tables S3 and S4. RybB expression and control plasmids have been described (17, 25, 55). Details of plasmids pFM58-1 (expressing RybBΔ1–9), pKP24-2 (MicF), pMB14 (pBAD-F14TMA), and pMB15 (pBAD-TMA) are found in *SI Appendix*.

SDS/PAGE and Western Blot Analysis of *Salmonella* Proteins. Culture samples were taken according to 1 OD_{600} and centrifuged for 4 min at 16,100 g at 4 °C, and pellets were resuspended in sample loading buffer to a final concentration of 0.01 OD_{600}/μL. Following denaturation for 5 min at 95 °C, 0.1/0.2 OD_{600} equivalents of sample were separated in small/large SDS gels, respectively. Western blot analysis and quantification followed previously published protocols (30). OmpX was detected as in (56). OmpA/C/D/F were detected with major porin antisera (1:50,000 dilution; provided by R. Misra, Tempe, AZ) and anti–rabbit-HRP (1:5,000 dilution; Sigma–Aldrich) as the secondary antibody.

RNA Isolation and Northern Blot. Total RNA was prepared and separated in 5 or 6% (vol/vol) polyacrylamide 8.3-M urea gels (5–15 μg of RNA per lane) and blotted as described (25). Membranes were hybridized at 42 °C with gene-specific [^{32}P] end-labeled DNA oligonucleotides, at 60 °C with an *ompC*-specific [^{32}P] PCR product (25) or with LNA probe 07150 at 37 °C in Rapid-hyb buffer (GE Healthcare). Detection of other *omp* mRNAs was done as de-

GENETICS

scribed (25). Hybridization signals were quantified on a FLA-3000 PhosphorImager (Fuji) with AIDA software (Raytest).

***gfp* Reporter Assays.** Target fusions to *gfp* were constructed as described by Urban and Vogel (30) and in *SI Appendix*, Tables S5. sRNA-dependent fusion regulation on Western blots was as described (30). For reporter activities in single cells (FACS), we used a Canto Flow Cytometer (no. 337175; BD Biosciences) equipped with a blue excitation source (air-cooled, 20-mW, solid-state 488-nm laser) to measure forward angle light scatter (FSC), side scatter (SSC) and cell fluorescence (FITC). Instrument settings were in logarithmic mode (FSC-H: 516, SSC-A: 626; and FITC-A: 962). GFP fluorescence intensity was calculated from 30,000 events (maximum threshold of 10,000 events per second) of triplicate samples, using FCS Express (De Novo Software). Strains were grown for 12 h after fresh inoculation, and 1 mL of culture was centrifuged for 2 min at 7,500 × *g* at room temperature. Pellets were resuspended in PBS (pH 7.4) containing 2% (wt/vol) paraformaldehyde, kept in the dark at 4 °C (≤5 d), and diluted 250-fold in 1× PBS immediately before FACS analysis.

ACKNOWLEDGMENTS. We thank F. Seifert for technical assistance, R. Misra (Tempe, AZ) and D. Linke (Tübingen, Germany) for porin antisera, V. Pfeiffer for plasmid construction, F. Darfeuille (Université de Bordeaux, France) for LNA synthesis, This work was supported by a European Molecular Biology Organization long-term fellowship (to M.B.) and by funds from the Deutsche Forschungsgemeinschaft Priority Program SPP1258 *Sensory and Regulatory RNAs in Prokaryotes* (to J.V.).

1. Waters LS, Storz G (2009) Regulatory RNAs in bacteria. *Cell* 136:615–628.
2. Bartel DP (2009) MicroRNAs: Target recognition and regulatory functions. *Cell* 136: 215–233.
3. Papenfort K, Vogel J (2009) Multiple target regulation by small noncoding RNAs rewires gene expression at the post-transcriptional level. *Res Microbiol* 160:278–287.
4. Massé E, Vanderpool CK, Gottesman S (2005) Effect of RyhB small RNA on global iron use in Escherichia coli. *J Bacteriol* 187:6962–6971.
5. Lease RA, Smith D, McDonough K, Belfort M (2004) The small noncoding DsrA RNA is an acid resistance regulator in Escherichia coli. *J Bacteriol* 186:6179–6185.
6. Boysen A, Møller-Jensen J, Kallipolitis B, Valentin-Hansen P, Overgaard M (2010) Translational regulation of gene expression by an anaerobically induced small noncoding RNA in Escherichia coli. *J Biol Chem* 285:10690–10702.
7. Altuvia S, Weinstein-Fischer D, Zhang A, Postow L, Storz G (1997) A small, stable RNA induced by oxidative stress: Role as a pleiotropic regulator and antimutator. *Cell* 90: 43–53.
8. Valentin-Hansen P, Eriksen M, Udesen C (2004) The bacterial Sm-like protein Hfq: A key player in RNA transactions. *Mol Microbiol* 51:1525–1533.
9. Zhang A, et al. (2003) Global analysis of small RNA and mRNA targets of Hfq. *Mol Microbiol* 50:1111–1124.
10. Sittka A, et al. (2008) Deep sequencing analysis of small noncoding RNA and mRNA targets of the global post-transcriptional regulator, Hfq. *PLoS Genet* 4:e1000163.
11. Vogel J (2009) A rough guide to the non-coding RNA world of Salmonella. *Mol Microbiol* 71:1–11.
12. Schmidt M, Zheng P, Delihas N (1995) Secondary structures of Escherichia coli antisense micF RNA, the 5′-end of the target ompF mRNA, and the RNA/RNA duplex. *Biochemistry* 34:3621–3631.
13. Møller T, Franch T, Udesen C, Gerdes K, Valentin-Hansen P (2002) Spot 42 RNA mediates discoordinate expression of the E. coli galactose operon. *Genes Dev* 16: 1696–1706.
14. Kawamoto H, Koide Y, Morita T, Aiba H (2006) Base-pairing requirement for RNA silencing by a bacterial small RNA and acceleration of duplex formation by Hfq. *Mol Microbiol* 61:1013–1022.
15. Wagner EG, Darfeuille F (2006) Small regulatory RNAs in bacteria. *Small RNAs: Analysis and Regulatory Functions*, eds Nellen W, Hamann C (Springer, Berlin), pp 1–29.
16. Pfeiffer V, Papenfort K, Lucchini S, Hinton JC, Vogel J (2009) Coding sequence targeting by MicC RNA reveals bacterial mRNA silencing downstream of translational initiation. *Nat Struct Mol Biol* 16:840–846.
17. Bouvier M, Sharma CM, Mika F, Nierhaus KH, Vogel J (2008) Small RNA binding to 5′ mRNA coding region inhibits translational initiation. *Mol Cell* 32:827–837.
18. Sharma CM, Darfeuille F, Plantinga TH, Vogel J (2007) A small RNA regulates multiple ABC transporter mRNAs by targeting C/A-rich elements inside and upstream of ribosome-binding sites. *Genes Dev* 21:2804–2817.
19. Vecerek B, Moll I, Bläsi U (2007) Control of Fur synthesis by the non-coding RNA RyhB and iron-responsive decoding. *EMBO J* 26:965–975.
20. Holmqvist E, et al. (2010) Two antisense RNAs target the transcriptional regulator CsgD to inhibit curli synthesis. *EMBO J* 29:1840–1850.
21. Desnoyers G, Morissette A, Prévost K, Massé E (2009) Small RNA-induced differential degradation of the polycistronic mRNA iscRSUA. *EMBO J* 28:1551–1561.
22. Guillier M, Gottesman S (2008) The 5′ end of two redundant sRNAs is involved in the regulation of multiple targets, including their own regulator. *Nucleic Acids Res* 36: 6781–6794.
23. Chen S, Zhang A, Blyn LB, Storz G (2004) MicC, a second small-RNA regulator of Omp protein expression in Escherichia coli. *J Bacteriol* 186:6689–6697.
24. Durand S, Storz G (2010) Reprogramming of anaerobic metabolism by the FnrS small RNA. *Mol Microbiol* 75:1215–1231.
25. Papenfort K, et al. (2006) SigmaE-dependent small RNAs of Salmonella respond to membrane stress by accelerating global omp mRNA decay. *Mol Microbiol* 62: 1674–1688.
26. Johansen J, Rasmussen AA, Overgaard M, Valentin-Hansen P (2006) Conserved small non-coding RNAs that belong to the sigmaE regulon: Role in down-regulation of outer membrane proteins. *J Mol Biol* 364:1–8.
27. Thompson KM, Rhodius VA, Gottesman S (2007) SigmaE regulates and is regulated by a small RNA in Escherichia coli. *J Bacteriol* 189:4243–4256.
28. Mutalik VK, Nonaka G, Ades SE, Rhodius VA, Gross CA (2009) Promoter strength properties of the complete sigma E regulon of Escherichia coli and Salmonella enterica. *J Bacteriol* 191:7279–7287.
29. Rhodius VA, Suh WC, Nonaka G, West J, Gross CA (2006) Conserved and variable functions of the sigmaE stress response in related genomes. *PLoS Biol* 4:e2.
30. Urban JH, Vogel J (2007) Translational control and target recognition by Escherichia coli small RNAs in vivo. *Nucleic Acids Res* 35:1018–1037.
31. Rehmsmeier M, Steffen P, Hochsmann M, Giegerich R (2004) Fast and effective prediction of microRNA/target duplexes. *RNA* 10:1507–1517.
32. Brantl S (2007) Regulatory mechanisms employed by cis-encoded antisense RNAs. *Curr Opin Microbiol* 10:102–109.
33. Wagner EG, Altuvia S, Romby P (2002) Antisense RNAs in bacteria and their genetic elements. *Adv Genet* 46:361–398.
34. Malmgren C, Engdahl HM, Romby P, Wagner EG (1996) An antisense/target RNA duplex or a strong intramolecular RNA structure 5′ of a translation initiation signal blocks ribosome binding: the case of plasmid R1. *RNA* 2:1022–1032.
35. Mizuno T, Chou MY, Inouye M (1984) A unique mechanism regulating gene expression: Translational inhibition by a complementary RNA transcript (micRNA). *Proc Natl Acad Sci USA* 81:1966–1970.
36. Friedman RC, Farh KK, Burge CB, Bartel DP (2009) Most mammalian mRNAs are conserved targets of microRNAs. *Genome Res* 19:92–105.
37. Morita T, Mochizuki Y, Aiba H (2006) Translational repression is sufficient for gene silencing by bacterial small noncoding RNAs in the absence of mRNA destruction. *Proc Natl Acad Sci USA* 103:4858–4863.
38. Morita T, Maki K, Aiba H (2005) RNase E-based ribonucleoprotein complexes: Mechanical basis of mRNA destabilization mediated by bacterial noncoding RNAs. *Genes Dev* 19:2176–2186.
39. Vogel J, Wagner EG (2007) Target identification of small noncoding RNAs in bacteria. *Curr Opin Microbiol* 10:262–270.
40. Yusupova GZ, Yusupov MM, Cate JH, Noller HF (2001) The path of messenger RNA through the ribosome. *Cell* 106:233–241.
41. Hüttenhofer A, Noller HF (1994) Footprinting mRNA-ribosome complexes with chemical probes. *EMBO J* 13:3892–3901.
42. Beyer D, Skripkin E, Wadzack J, Nierhaus KH (1994) How the ribosome moves along the mRNA during protein synthesis. *J Biol Chem* 269:30713–30717.
43. Takyar S, Hickerson RP, Noller HF (2005) mRNA helicase activity of the ribosome. *Cell* 120:49–58.
44. Celesnik H, Deana A, Belasco JG (2007) Initiation of RNA decay in Escherichia coli by 5′ pyrophosphate removal. *Mol Cell* 27:79–90.
45. Emory SA, Bouvet P, Belasco JG (1992) A 5′-terminal stem-loop structure can stabilize mRNA in Escherichia coli. *Genes Dev* 6:135–148.
46. Caron MP, Lafontaine DA, Massé E (2010) Small RNA-mediated regulation at the level of transcript stability. *RNA Biol* 7:140–144.
47. Elgart V, Jia T, Kulkarni R (2010) Quantifying mRNA synthesis and decay rates using small RNAs. *Biophys J* 98:2780–2784.
48. Massé E, Escorcia FE, Gottesman S (2003) Coupled degradation of a small regulatory RNA and its mRNA targets in Escherichia coli. *Genes Dev* 17:2374–2383.
49. Udekwu KI, et al. (2005) Hfq-dependent regulation of OmpA synthesis is mediated by an antisense RNA. *Genes Dev* 19:2355–2366.
50. Coornaert A, et al. (2010) MicA sRNA links the PhoP regulon to cell envelope stress. *Mol Microbiol* 76:467–479.
51. Bossi L, Figueroa-Bossi N (2007) A small RNA downregulates LamB maltoporin in Salmonella. *Mol Microbiol* 65:799–810.
52. Udekwu KI, Wagner EG (2007) Sigma E controls biogenesis of the antisense RNA MicA. *Nucleic Acids Res* 35:1279–1288.
53. Brennan RG, Link TM (2007) Hfq structure, function and ligand binding. *Curr Opin Microbiol* 10:125–133.
54. Coleman J, Green PJ, Inouye M (1984) The use of RNAs complementary to specific mRNAs to regulate the expression of individual bacterial genes. *Cell* 37:429–436.
55. Sittka A, Pfeiffer V, Tedin K, Vogel J (2007) The RNA chaperone Hfq is essential for the virulence of Salmonella typhimurium. *Mol Microbiol* 63:193–217.
56. Papenfort K, et al. (2008) Systematic deletion of Salmonella small RNA genes identifies CyaR, a conserved CRP-dependent riboregulator of OmpX synthesis. *Mol Microbiol* 68:890–906.